THE JOURNAL OF PHYSICAL CHEMISTRY Letters

Letter

pubs.acs.org/JPCL

Specific Monitoring of Excited-State Symmetry Breaking by Femtosecond Broadband Fluorescence Upconversion Spectroscopy

Joseph S. Beckwith,[†] Arnulf Rosspeintner,[†] Giuseppe Licari,[†] Markus Lunzer,[‡] Brigitte Holzer,[‡] Johannes Fröhlich,[‡] and Eric Vauthey*[,†]

[†]Physical Chemistry Department, University of Geneva, Quai Ernest Ansermet 30, CH-1211 Geneva, Switzerland

[‡]Institute of Applied Synthetic Chemistry, TU Wien, Getreidemarkt 9/163OC, A-1060 Vienna, Austria

Supporting Information

ABSTRACT: Most quadrupolar molecules designed for large two-photon absorption cross section have been shown to undergo symmetry breaking upon excitation to the S_1 state. This was originally deduced from their strong fluorescence solvatochromism and later visualized in real time using transient infrared spectroscopy. For molecules not containing clear IR marker modes, however, a specific real-time observation of the symmetry breaking process remains lacking. Here we show that this process can be resolved using broadband fluorescence upconversion spectroscopy by monitoring the instantaneous emission transition dipole moment. This approach is illustrated with measurements performed on two quadrupolar molecules, with only one of them undergoing excited-state symmetry breaking in polar solvents.

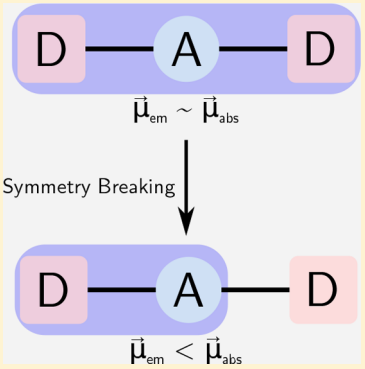

Molecules that have a large two-photon absorption cross section, $\sigma^{(2)}$, are of interest for a variety of applications that include bioimaging, photopolymerization, photodynamic therapy, and data storage.[1−13] Large $\sigma^{(2)}$ values are associated with large changes of electric quadrupolar or octupolar moments upon excitation,[14−16] and thus most chromophores with large $\sigma^{(2)}$ values synthesized to date contain several electron donor and acceptor (D and A, respectively) units arranged in conjugated chromophores of DA_n or AD_n type (where n generally equals 2 or 3). The electronic ground state of these molecules is well understood due to a range of investigations that have successfully related their multipolar character, symmetry, one-photon absorption spectra and their $\sigma^{(2)}$ cross sections.[17−23] For a long time, their excited states presented considerable confusion: Whereas the electronic absorption spectra of AD_n and DA_n molecules usually present little solvent dependence, to be anticipated for purely quadrupolar or octupolar electronic states, the fluorescence spectra display a strong solvatochromism reminiscent of a dipolar S_1 state.[18−20,24,25] This phenomenon was rationalized using an essential-state model in which structural or solvent fluctuations break the symmetry of the excited state.[26−28]

A real-time observation of this symmetry breaking was lacking until recently because transient electronic absorption spectroscopy does not provide a clear spectroscopic signature of this process.[29,30] However, clear real-time observation of the symmetry breaking was achieved using time-resolved IR spectroscopy to monitor specific vibrational modes located in the two branches of quadrupolar molecules.[31−34] These investigations revealed that, for these molecules at least, symmetry breaking is driven by the environment, more specifically by differences in the instantaneous orientation of the solvent molecules around the two arms of the molecule and that their symmetry-breaking dynamics occur on similar time scales as those of solvent motion. The asymmetry of the instantaneous solvent orientation also plays a key role in photoinduced symmetry-breaking charge-separation processes between two identical molecules.[35−41] Here, however, symmetry breaking can be easily identified by the presence of absorption bands of the resulting anionic and cationic species.

However, for quadrupolar molecules without specific IR markers, a real-time observation of symmetry breaking remains lacking. Kim et al. applied broadband fluorescence upconversion spectroscopy (FLUPS)[42,43] to track the peak position of the emission spectrum.[44] However, the time-dependent shift of the emission band also reports on solvent relaxation.[45] Because

Chart 1. Structures of the Two DAD Molecules Investigated

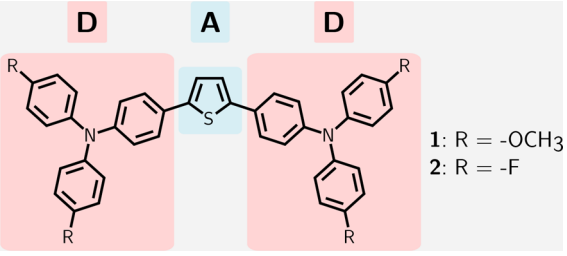

Received: October 17, 2017
Accepted: November 16, 2017
Published: November 16, 2017

DOI: 10.1021/acs.jpclett.7b02754
J. Phys. Chem. Lett. 2017, 8, 5878−5883

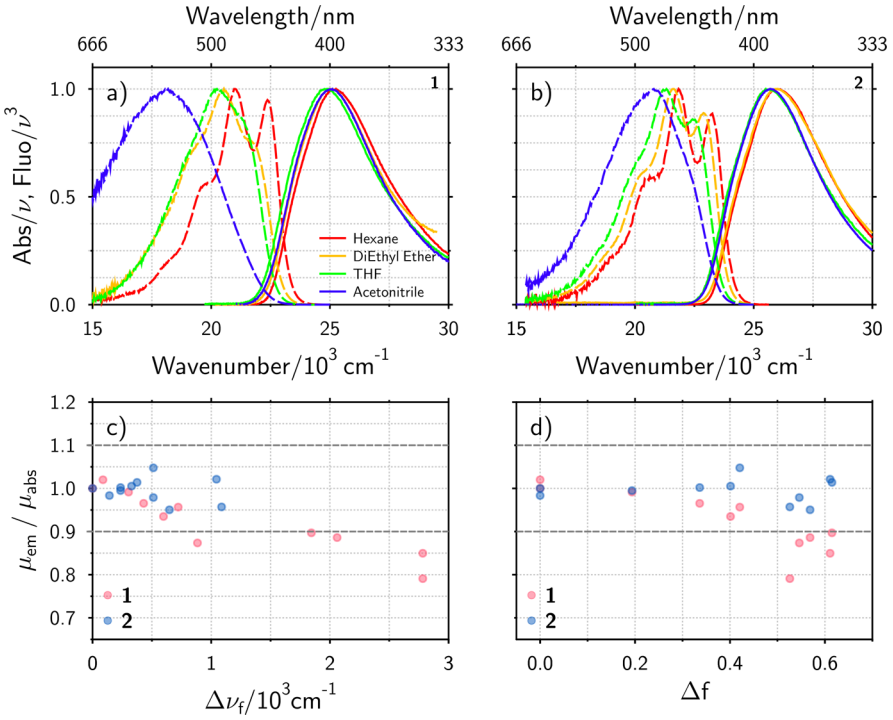

Figure 1. Solvent dependence of the electronic absorption and fluorescence spectra of (a) **1** and (b) **2** in the transition dipole moment representation.[46] Ratio of the emission and absorption transition dipole moments of **1** and **2** versus (c) the shift of the fluorescence band maximum relative to hexane, $\Delta\nu_f$, and (d) the solvent polarity function, Δf. The μ_{em}/μ_{abs} ratios are referred to those in hexane that have been set equal to 1. The dashed lines represent the ±0.1 limit of error.

quadrupolar states are also stabilized by dipolar solvation,[26] it is not clear whether the shift of the emission band due to solvent relaxation around the quadrupolar excited state can be unambiguously distinguished from that due to symmetry breaking from a quadupolar to a dipolar excited state. Because both processes may occur on similar time scales, it is, in principle, not possible to distinguish between where the solvation of the quadrupole ends and the symmetry-breaking process begins, meaning that the tracking of the peak position is not specific to the observation of symmetry breaking in real-time.

Here we propose a different approach, also based on FLUPS, to visualize excited-state symmetry breaking in quadrupolar molecules. Instead of tracking the temporal evolution of the $S_1 \rightarrow S_0$ transition energy, we look at how the size of the $S_1 \rightarrow S_0$ transition dipole moment, $\mu_{em} = |\vec{\mu}_{em}|$, changes with time. The one-photon and two-photon absorption spectra of DA_n or AD_n molecules can be qualitatively well explained in terms of an excitonic model, where each DA branch is a chromophoric unit with a local transition dipole, $\vec{\mu}_{DA}$.[20] In the case of a linear two-branch molecule, the transition to the lowest singlet excitonic state is one-photon allowed, but two-photon forbidden, and the size of its dipole moment, μ_{abs}, is approximately $\sqrt{2}\mu_{DA}$. Similarly, the transition to the S_2 state is one photon forbidden but two-photon allowed. According to this model, the dipole moment for the $S_1 \rightarrow S_0$ emission should be equal to μ_{abs} as long as the S_1 state remains symmetric and the excitation is equally distributed over the two branches of the molecule. However, in the case of a complete symmetry breaking with the excitation entirely localized on one branch, the emission transition dipole should be reduced to $\mu_{em} \approx \mu_{abs}/\sqrt{2}$. Therefore, time resolving μ_{em} can be anticipated to be a viable approach for monitoring symmetry breaking in real time.

To test this idea, we have measured the time dependence of the emission transition dipole moment of two molecules, **1** and **2** (Chart 1), using FLUPS. These molecules were developed for applications in two-photon induced polymerization and are composed of a central thiophene core flanked by two triphenylamines with either methoxy (**1**) or fluorine (**2**) substituents, conferring to the end-cap units a very different electron-donating strength. As a consequence, **1** is expected to have much stronger DAD character than **2** and thus excited-state symmetry breaking is only expected for **1**.

Although these two molecules are not strictly linear, the relative intensities of their $S_1 \leftarrow S_0$ and $S_2 \leftarrow S_0$ bands in the one- and two-photon absorption spectra are fully consistent with those expected for linear quadrupolar molecules according to the excitonic model (Figure S6).[20,47,48] The solvent dependence of their stationary absorption and emission spectra is shown in Figure 1a,b. Whereas the $S_1 \leftarrow S_0$ absorption band is broad and structureless in all solvents, the fluorescence band in nonpolar solvents is far from mirror image and exhibits a distinct vibrational progression. Such an absence of mirror-image relationship is typical of conjugated polyaryl molecules and can be explained by the strong increase in the barrier for torsion around the single bonds between the aryl subunits upon excitation.[49−51] Consequently, the large width of the absorption band arises from torsional disorder in the ground state, whereas the structured fluorescence band reflects a more rigid planar geometry of the S_1 state favored by conjugation. This is confirmed by quantum-chemical calculations of the energy of S_0 and S_1 states of **1** and **2** as a function of the dihedral angle between the central thiophene and an adjacent phenyl unit (Figures S28 and S29). Figure 1 also reveals an equally weak solvatochromism of the absorption spectrum of **1** and **2**, in agreement with a quadrupolar ground state and Franck−

DOI: 10.1021/acs.jpclett.7b02754
J. Phys. Chem. Lett. 2017, 8, 5878−5883

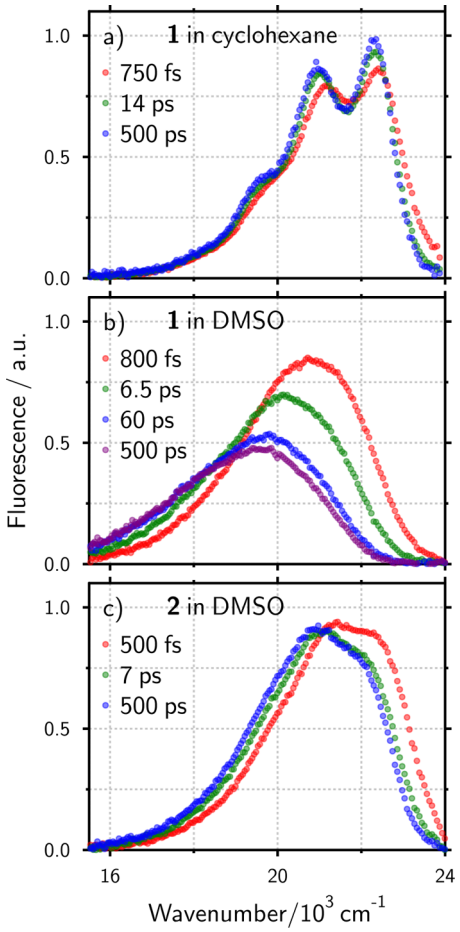

Figure 2. Transient emission spectra recorded at different time delays after excitation of **1** in (a) cyclohexane and (b) DMSO and (c) **2** in DMSO.

Condon S_1 state. The absorption maximum shows a good correlation with the function $f(n^2) = 2(n^2 - 1)/(2n^2 + 1)$, where n is the refractive index, indicating that the absorption solvatochromism is dominated by dispersion interactions (Figure S2). By contrast, the fluorescence solvatochromism is much more pronounced. Whereas a plot of the emission maximum of **2** versus the polarity function $\Delta f = 2(\epsilon - 1)/(2\epsilon + 1) - f(n^2)$, where ϵ is the static dielectric constant, is approximately linear, that for **1** shows a slope that increases with Δf (Figure S3). This can be explained by an increasing permanent dipole moment of the S_1 state with solvent polarity, suggesting a breaking of the symmetry of the S_1 state of **1** but not **2** in polar solvents.

Both μ_{abs} and μ_{em} were calculated from these spectra (see SI for details), and their ratio μ_{em}/μ_{abs} is plotted versus the shift of the fluorescence band maximum relative to hexane, $\Delta\nu_f$, and Δf in Figure 1c,d. Whereas this ratio remains between 0.9 and 1.1 for **2** in all solvents investigated, it is markedly smaller for **1** in the most polar solvents, indicative of symmetry breaking. However, this difference between **1** and **2** is not much greater than the error on μ_{em}/μ_{abs} (± 0.1). This error arises mostly from the difficulty to determine the absorption coefficient accurately when a limited amount of compound is available.[52]

These problems can be largely avoided by determining the temporal evolution of μ_{em}. Figure 2 shows FLUPS spectra recorded at different time delays after excitation of **1** in cyclohexane and DMSO as well as of **2** in DMSO. Both

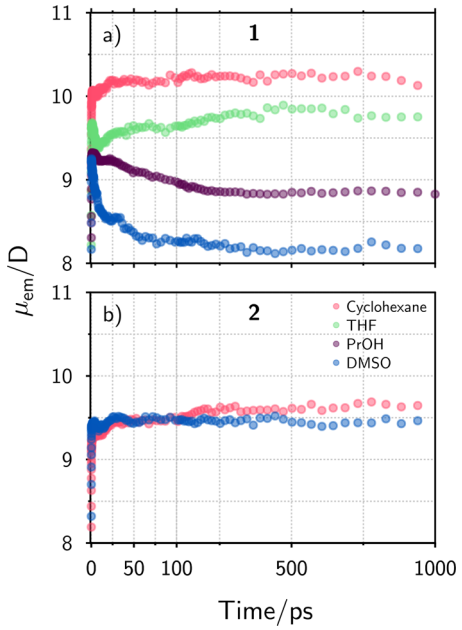

Figure 3. Time dependence of μ_{em} of (a) **1** in cyclohexane, propanol (PrOH), THF, and DMSO and (b) **2** in cyclohexane and DMSO. All traces are normalized to steady state value at long times. Note the change of linear axis at 100 ps.

molecules exhibit very similar fluorescence dynamics in cyclohexane: during the first 20 ps, the emission band narrows and shifts to lower frequencies and its vibrational structure develops (Figure 2a and Figure S14). These changes are assigned to the planarization of the molecules in the S_1 state.[49−51] Afterward, the spectral shape remains unchanged and the amplitude decays exponentially to zero on the 500 ps time scale, in good agreement with the fluorescence lifetime, τ_F, determined by time-correlated single photon counting (TCSPC, Table S1).

The time evolution of μ_{em} was determined by first dividing the FLUPS signal by $e^{-(t/\tau_F)}$ to correct for the population decay and by $\tilde{\nu}^3$, where $\tilde{\nu}$ is the wavenumber,[46] and second by calculating the square-rooted area of the resulting spectra (see the SI for details).

Figure 3 indicates that the time evolution of μ_{em} in cyclohexane is the same for both molecules and consists of an initial increase by ∼5% during the first 20 ps to a value that remains constant within the entire 0 to 1 ns time window of the experiment. This rise coincides with the initial spectral dynamics attributed to planarization and is interpreted as arising from the same process. This corroborates with quantum-chemical calculations that predict an increase in the transition dipole moment upon decreasing the dihedral angle between the central thiophene and an adjacent phenyl unit (Figures S28 and S29).

In DMSO, the fluorescence spectrum of **2** exhibits a ∼1000 cm^{-1} frequency downshift together with changes in the vibrational envelope during the first 10−15 ps after excitation. This is followed by an exponential decay on the 1 ns time scale, in agreement with the TCSPC fluorescence lifetime (Figure 2c). The initial spectral dynamics can be ascribed to both planarization and solvent relaxation. The time dependence of μ_{em} shows the initial rise assigned to planarization and then remains constant (Figure 3). By contrast, the fluorescence spectrum of **1** undergoes a significantly larger frequency

DOI: 10.1021/acs.jpclett.7b02754
J. Phys. Chem. Lett. 2017, 8, 5878−5883

downshift, ~1500 cm^{-1}, and a fast partial decrease in intensity before decaying with the 2.47 ns lifetime recorded by TCSPC (Figure 2b). Figure 3 reveals that this initial decrease in intensity is associated with a ~ 10% reduction of μ_{em}. This decay of μ_{em} can be reproduced with a biexponential function with 4.3 and 38 ps components of similar amplitude. This decrease in the transition dipole moment can be assigned to a change of the nature of the emitting state and hence to symmetry breaking. The fast decay component most probably reflects symmetry breaking brought about by solvation, in agreement with previous reports using time-resolved IR spectroscopy.[31−34] However, the 38 ps component exceeds by far the time scale of solvent motion[45] and could originate from structural relaxation occurring upon partial localization of the excitation on one branch, that is, upon redistribution of the electronic density on the two donor subunits. This slower process appears not only as a partial intensity decay of the emission band but also as a small, ~230 cm^{-1}, red shift. Symmetry breaking of **1** in polar solvents is further confirmed by similar measurements in PrOH, where μ_{em} also decays but only by ~5%. This weaker decrease of μ_{em} can be explained by a smaller extent of symmetry breaking of the excited state due to the lower polarity of this solvent. In the less polar THF, the solvent reaction field is apparently too weak for symmetry breaking to take place because no significant decrease in μ_{em} is observed.

These results confirm that the temporal variation of μ_{em} offers direct access to the symmetry breaking dynamics of the excited state and is a valuable alternative to time-resolved IR spectroscopy, especially for molecules such as those investigated here that do not contain vibrational markers localized on the two DA branches. Moreover, the amplitude of this change of μ_{em} reflects the extent of symmetry breaking. Because planarization of **1** and **2** should give approximately the same ~5% increase in transition dipole in all solvents, the actual decrease in μ_{em} upon symmetry breaking of **1** in DMSO should be ~15%. This value indicates that here symmetry breaking does not lead to a full localization of the excitation on one DA branch. If this were the case, then μ_{em} should decrease by ~40% according to quantum-chemical calculations of **1** and of its single-branch analogue (see SI for details) and by 30% according to the above-mentioned excitonic model.

We now consider whether symmetry breaking can be directly inferred from the dynamic Stokes shift of the fluorescence band. Figure 4 compares the changes of μ_{em} and of the peak position measured after excitation of **1** and **2** in various solvents. If the dynamic Stokes shift were a measure of the symmetry-breaking process, then the decrease in μ_{em} should be well-correlated with the change of peak position. As is shown by Figure 4, this is evidently not the case. For **2** in DMSO, there is a ~1000 cm^{-1} shift of the emission band but no change of μ_{em}. Equally, the ~800 cm^{-1} band shift of **1** in THF is not accompanied by a significant variation of μ_{em}, apart from that associated with planarization. The latter process leads to an increase in μ_{em} with frequency downshift, as better seen in cyclohexane. For **1** in DMSO, μ_{em} decreases in parallel with the frequency downshift of the emission. However, in PrOH, μ_{em} remains constant during an initial ~600 cm^{-1} band shift and only decreases during a further ~400 cm^{-1} shift.

Although the Stokes shift is the largest when symmetry breaking takes place, it does not only reflect this process. This confirms our initial argument that the fluorescence shift does not allow one to distinguish between where quadrupolar solvation ends and symmetry breaking begins.

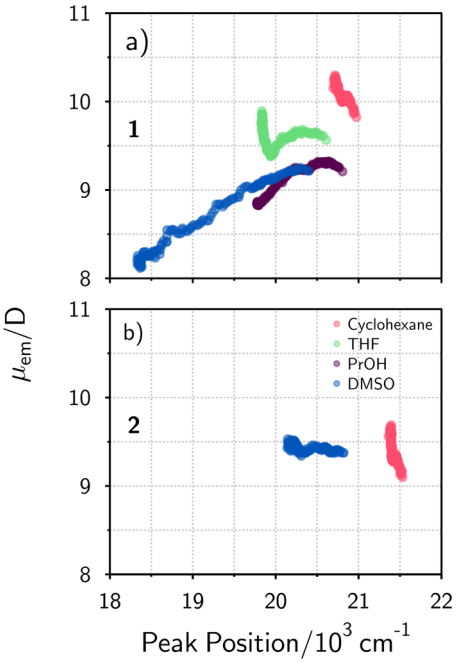

Figure 4. μ_{em} versus the peak position of the emission band of (a) **1** in cyclohexane, propanol (PrOH), THF, and DMSO, and (b) **2** in cyclohexane and DMSO.

In conclusion, we could show that the instantaneous μ_{em} is a sensitive reporter of symmetry breaking in the excited state and that this process can be specifically monitored in real time using broadband fluorescence upconversion spectroscopy. Additionally, our results reveal that the temporal shift of the fluorescence band cannot be used as a specific reporter on symmetry breaking and that its magnitude is not a well-suited guide for judging in which solvents symmetry breaking occurs. Such information can, in principle, be deduced from the μ_{em}/μ_{abs} ratio. However, the error on the absolute magnitude of μ_{abs} is usually large when having limited amount of compound, and thus monitoring its temporal change of μ_{em} is by far more reliable.

■ ASSOCIATED CONTENT

Supporting Information

The Supporting Information is available free of charge on the ACS Publications website at DOI: 10.1021/acs.jpclett.7b02754.

Description of the experimental procedures. Lineshape analysis of the steady-state spectra and transition dipole moment calculations. Comparison of one- and two-photon absorption spectra. Details of FLUPS data analysis. Additional FLUPS data. Quantum-chemical calculations. (PDF)

■ AUTHOR INFORMATION

Corresponding Author

*E-mail: eric.vauthey@unige.ch.

ORCID

Arnulf Rosspeintner: 0000-0002-1828-5206

Brigitte Holzer: 0000-0003-4400-9827

Eric Vauthey: 0000-0002-9580-9683

DOI: 10.1021/acs.jpclett.7b02754
J. Phys. Chem. Lett. 2017, 8, 5878−5883

Notes

The authors declare no competing financial interest.

■ ACKNOWLEDGMENTS

We thank the Fonds National Suisse de la Recherche Scientifique (project no. 200020-165890) as well as the University of Geneva for financial support.

■ REFERENCES

(1) Denk, W.; Strickler, J. H.; Webb, W. W. Two-Photon Laser Scanning Fluorescence Microscopy. *Science* **1990**, *248*, 73−76.
(2) Albota, M.; Beljonne, D.; Brédas, J.-L.; Ehrlich, J. E.; Fu, J.-Y.; Heikal, A. A.; Hess, S. E.; Kogej, T.; Levin, M. D.; Marder, S. R.; et al. Design of Organic Molecules with Large Two-Photon Absorption Cross Sections. *Science* **1998**, *281*, 1653−1656.
(3) Kawata, S.; Sun, H.-B.; Tanaka, T.; Takada, K. Finer Features for Functional Microdevices. *Nature* **2001**, *412*, 697−698.
(4) Zhou, W.; Kuebler, S. M.; Braun, K. L.; Yu, T.; Cammack, J. K.; Ober, C. K.; Perry, J. W.; Marder, S. R. An Efficient Two-Photon-Generated Photoacid Applied to Positive-Tone 3D Microfabrication. *Science* **2002**, *296*, 1106−1109.
(5) Brown, S. B.; Brown, E. A.; Walker, I. The Present and Future Role of Photodynamic Therapy in Cancer Treatment. *Lancet Oncol.* **2004**, *5*, 497−508.
(6) Le Droumaguet, C.; Mongin, O.; Werts, M. H. V.; Blanchard-Desce, M. Towards "Smart" Multiphoton Fluorophores: Strongly Solvatochromic Probes for Two- Photon Sensing of Micropolarity. *Chem. Commun.* **2005**, *0*, 2802−2804.
(7) Goodwin, A. P.; Mynar, J. L.; Ma, Y.; Fleming, G. R.; Fréchet, J. M. J. Synthetic Micelle Sensitive to IR Light via a Two-Photon Process. *J. Am. Chem. Soc.* **2005**, *127*, 9952−9953.
(8) Lee, K.-S.; Yang, D.-Y.; Park, S. H.; Kim, R. H. Recent Developments in the Use of Two-Photon Polymerization in Precise 2D and 3D Microfabrications. *Polym. Adv. Technol.* **2006**, *17*, 72−82.
(9) LaFratta, C.; Fourkas, J.; Baldacchini, T.; Farrer, R. Multiphoton Fabrication. *Angew. Chem., Int. Ed.* **2007**, *46*, 6238−6258.
(10) Walker, E.; Rentzepis, P. M. Two-Photon Technology: A New Dimension. *Nat. Photonics* **2008**, *2*, 406−408.
(11) Li, Z.; Siklos, M.; Pucher, N.; Cicha, K.; Ajami, A.; Husinsky, W.; Rosspeintner, A.; Vauthey, E.; Gescheidt, G.; Stampfl, J.; et al. Synthesis and Structure-Activity Relationship of Several Aromatic Ketone-Based Two-Photon Initiators. *J. Polym. Sci., Part A: Polym. Chem.* **2011**, *49*, 3688−3699.
(12) Kawakami, R.; Sawada, K.; Sato, A.; Hibi, T.; Kozawa, Y.; Sato, S.; Yokoyama, H.; Nemoto, T. Visualizing Hippocampal Neurons with *in Vivo* Two-Photon Microscopy Using a 1030 Nm Picosecond Pulse Laser. *Sci. Rep.* **2013**, *3*, srep01014.
(13) Obata, K.; El-Tamer, A.; Koch, L.; Hinze, U.; Chichkov, B. N. High-Aspect 3D Two-Photon Polymerization Structuring with Widened Objective Working Range (WOW-2PP). *Light: Sci. Appl.* **2013**, *2*, e116.
(14) Rumi, M.; Ehrlich, J. E.; Heikal, A. A.; Perry, J. W.; Barlow, S.; Hu, Z.; McCord-Maughon, D.; Parker, T. C.; Röckel, H.; Thayumanavan, S.; et al. Structure-Property Relationships for Two-Photon Absorbing Chromophores: Bis-Donor Diphenylpolyene and Bis(Styryl)Benzene Derivatives. *J. Am. Chem. Soc.* **2000**, *122*, 9500−9510.
(15) Masunov, A.; Tretiak, S. Prediction of Two-Photon Absorption Properties for Organic Chromophores Using Time-Dependent Density-Functional Theory. *J. Phys. Chem. B* **2004**, *108*, 899−907.
(16) Terenziani, F.; Katan, C.; Badaeva, E.; Tretiak, S.; Blanchard-Desce, M. Enhanced Two-Photon Absorption of Organic Chromophores: Theoretical and Experimental Assessments. *Adv. Mater.* **2008**, *20*, 4641−4678.
(17) Chung, S.-J.; Kim, K.-S.; Lin, T.-C.; He, G. S.; Swiatkiewicz, J.; Prasad, P. N. Cooperative Enhancement of Two-Photon Absorption in Multi-Branched Structures. *J. Phys. Chem. B* **1999**, *103*, 10741−10745.
(18) Strehmel, B.; Sarker, A. M.; Detert, H. The Influence of σ and π Acceptors on Two-Photon Absorption and Solvatochromism of Dipolar and Quadrupolar Unsaturated Organic Compounds. *ChemPhysChem* **2003**, *4*, 249−259.
(19) Woo, H. Y.; Liu, B.; Kohler, B.; Korystov, D.; Mikhailovsky, A.; Bazan, G. C. Solvent Effects on the Two-Photon Absorption of Distyrylbenzene Chromophores. *J. Am. Chem. Soc.* **2005**, *127*, 14721−14729.
(20) Katan, C.; Terenziani, F.; Mongin, O.; Werts, M. H. V.; Porrès, L.; Pons, T.; Mertz, J.; Tretiak, S.; Blanchard-Desce, M. Effects of (Multi)Branching of Dipolar Chromophores on Photophysical Properties and Two-Photon Absorption. *J. Phys. Chem. A* **2005**, *109*, 3024−3037.
(21) Chung, S.-J.; Zheng, S.; Odani, T.; Beverina, L.; Fu, J.; Padilha, L. A.; Biesso, A.; Hales, J. M.; Zhan, X.; Schmidt, K.; et al. Extended Squaraine Dyes with Large Two-Photon Absorption Cross-Sections. *J. Am. Chem. Soc.* **2006**, *128*, 14444−14445.
(22) Rebane, A.; Drobizhev, M.; Makarov, N. S.; Beuerman, E.; Haley, J. E.; Krein, D. M.; Burke, A. R.; Flikkema, J. L.; Cooper, T. M. Relation between Two-Photon Absorption and Dipolar Properties in a Series of Fluorenyl-Based Chromophores with Electron Donating or Electron Withdrawing Substituents. *J. Phys. Chem. A* **2011**, *115*, 4255−4262.
(23) Pawlicki, M.; Collins, H.; Denning, R.; Anderson, H. Two-Photon Absorption and the Design of Two-Photon Dyes. *Angew. Chem., Int. Ed.* **2009**, *48*, 3244−3266.
(24) Verbouwe, W.; Van der Auweraer, M.; De Schryver, F. C.; Piet, J. J.; Warman, J. M. Excited State Localization or Delocalization in C3-Symmetric Amino-Substituted Triphenylbenzene Derivatives. *J. Am. Chem. Soc.* **1998**, *120*, 1319−1324.
(25) Amthor, S.; Lambert, C.; Dümmler, S.; Fischer, I.; Schelter, J. Excited Mixed-Valence States of Symmetrical Donor-Acceptor-Donor π Systems. *J. Phys. Chem. A* **2006**, *110*, 5204−5214.
(26) Terenziani, F.; Painelli, A.; Katan, C.; Charlot, M.; Blanchard-Desce, M. Charge Instability in Quadrupolar Chromophores: Symmetry Breaking and Solvatochromism. *J. Am. Chem. Soc.* **2006**, *128*, 15742−15755.
(27) Terenziani, F.; Sissa, C.; Painelli, A. Symmetry Breaking in Octupolar Chromophores: Solvatochromism and Electroabsorption. *J. Phys. Chem. B* **2008**, *112*, 5079−5087.
(28) Sissa, C.; Parthasarathy, V.; Drouin-Kucma, D.; Werts, M. H. V.; Blanchard-Desce, M.; Terenziani, F. The Effectiveness of Essential-State Models in the Description of Optical Properties of Branched Push−pull Chromophores. *Phys. Chem. Chem. Phys.* **2010**, *12*, 11715−11727.
(29) Zoon, P. D.; van Stokkum, I. H. M.; Parent, M.; Mongin, O.; Blanchard-Desce, M.; Brouwer, A. M. Fast Photo-Processes in Triazole-Based Push−pull Systems. *Phys. Chem. Chem. Phys.* **2010**, *12*, 2706−2715.
(30) Carlotti, B.; Benassi, E.; Spalletti, A.; Fortuna, C. G.; Elisei, F.; Barone, V. Photoinduced Symmetry-Breaking Intramolecular Charge Transfer in a Quadrupolar Pyridinium Derivative. *Phys. Chem. Chem. Phys.* **2014**, *16*, 13984−13994.
(31) Dereka, B.; Rosspeintner, A.; Li, Z.; Liska, R.; Vauthey, E. Direct Visualization of Excited-State Symmetry Breaking Using Ultrafast Time-Resolved Infrared Spectroscopy. *J. Am. Chem. Soc.* **2016**, *138*, 4643−4649.
(32) Dereka, B.; Rosspeintner, A.; Krzeszewski, M.; Gryko, D. T.; Vauthey, E. Symmetry-Breaking Charge Transfer and Hydrogen Bonding: Toward Asymmetrical Photochemistry. *Angew. Chem., Int. Ed.* **2016**, *55*, 15624−15628.
(33) Dereka, B.; Koch, M.; Vauthey, E. Looking at Photoinduced Charge Transfer Processes in the IR: Answers to Several Long-Standing Questions. *Acc. Chem. Res.* **2017**, *50*, 426−434.
(34) Dereka, B.; Vauthey, E. Solute−Solvent Interactions and Excited-State Symmetry Breaking: Beyond the Dipole−Dipole and the Hydrogen-Bond Interactions. *J. Phys. Chem. Lett.* **2017**, *8*, 3927−3932.

DOI: 10.1021/acs.jpclett.7b02754
J. Phys. Chem. Lett. 2017, 8, 5878−5883

(35) Piet, J. J.; Schuddeboom, W.; Wegewijs, B. R.; Grozema, F. C.; Warman, J. M. Symmetry Breaking in the Relaxed S1 Excited State of Bianthryl Derivatives in Weakly Polar Solvents. *J. Am. Chem. Soc.* **2001**, *123*, 5337−5347.
(36) Giaimo, J. M.; Gusev, A. V.; Wasielewski, M. R. Excited-State Symmetry Breaking in Cofacial and Linear Dimers of a Green Perylenediimide Chlorophyll Analogue Leading to Ultrafast Charge Separation. *J. Am. Chem. Soc.* **2002**, *124*, 8530−8531.
(37) Holman, M. W.; Yan, P.; Adams, D. M.; Westenhoff, S.; Silva, C. Ultrafast Spectroscopy of the Solvent Dependence of Electron Transfer in a Perylenebisimide Dimer. *J. Phys. Chem. A* **2005**, *109*, 8548−8552.
(38) Lewis, F. D.; Daublain, P.; Zhang, L.; Cohen, B.; Vura-Weis, J.; Wasielewski, M. R.; Shafirovich, V.; Wang, Q.; Raytchev, M.; Fiebig, T. Reversible Bridge-Mediated Excited-State Symmetry Breaking in Stilbene-Linked DNA Dumbbells. *J. Phys. Chem. B* **2008**, *112*, 3838−3843.
(39) Markovic, V.; Villamaina, D.; Barabanov, I.; Lawson Daku, L. M.; Vauthey, E. Photoinduced Symmetry-Breaking Charge Separation: The Direction of the Charge Transfer. *Angew. Chem., Int. Ed.* **2011**, *50*, 7596−7598.
(40) Vauthey, E. Photoinduced Symmetry-Breaking Charge Separation. *ChemPhysChem* **2012**, *13*, 2001−2011.
(41) Wu, Y.; Young, R. M.; Frasconi, M.; Schneebeli, S. T.; Spenst, P.; Gardner, D. M.; Brown, K. E.; Würthner, F.; Stoddart, J. F.; Wasielewski, M. R. Ultrafast Photoinduced Symmetry-Breaking Charge Separation and Electron Sharing in Perylenediimide Molecular Triangles. *J. Am. Chem. Soc.* **2015**, *137*, 13236−13239.
(42) Zhang, X.-X.; Würth, C.; Zhao, L.; Resch-Genger, U.; Ernsting, N. P.; Sajadi, M. Femtosecond Broadband Fluorescence Upconversion Spectroscopy: Improved Setup and Photometric Correction. *Rev. Sci. Instrum.* **2011**, *82*, 063108.
(43) Gerecke, M.; Bierhance, G.; Gutmann, M.; Ernsting, N. P.; Rosspeintner, A. Femtosecond Broadband Fluorescence Upconversion Spectroscopy: Spectral Coverage versus Efficiency. *Rev. Sci. Instrum.* **2016**, *87*, 053115.
(44) Kim, W.; Sung, J.; Grzybowski, M.; Gryko, D. T.; Kim, D. Modulation of Symmetry-Breaking Intramolecular Charge-Transfer Dynamics Assisted by Pendant Side Chains in π-Linkers in Quadrupolar Diketopyrrolopyrrole Derivatives. *J. Phys. Chem. Lett.* **2016**, *7*, 3060−3066.
(45) Horng, M. L.; Gardecki, J. A.; Papazyan, A.; Maroncelli, M. Subpicosecond Measurements of Polar Solvation Dynamics: Coumarin 153 Revisited. *J. Phys. Chem.* **1995**, *99*, 17311−17337.
(46) Angulo, G.; Grampp, G.; Rosspeintner, A. Recalling the Appropriate Representation of Electronic Spectra. *Spectrochim. Acta, Part A* **2006**, *65*, 727−731.
(47) Friese, D. H.; Mikhaylov, A.; Krzeszewski, M.; Poronik, Y. M.; Rebane, A.; Ruud, K.; Gryko, D. T. Pyrrolo[3,2-b]Pyrroles—From Unprecedented Solvatofluorochromism to Two-Photon Absorption. *Chem. - Eur. J.* **2015**, *21*, 18364−18374.
(48) Lukasiewicz, Å. G.; Ryu, H. G.; Mikhaylov, A.; Azarias, C.; Banasiewicz, M.; Kozankiewicz, B.; Ahn, K. H.; Jacquemin, D.; Rebane, A.; Gryko, D. T. Symmetry Breaking in Pyrrolo[3,2-b]pyrroles: Synthesis, Solvatofluorochromism and Two-photon Absorption. *Chem. - Asian J.* **2017**, *12*, 1736−1748.
(49) Sluch, M. I.; Godt, A.; Bunz, U. H. F.; Berg, M. A. Excited-State Dynamics of Oligo(p-Phenyleneethynylene): Quadratic Coupling and Torsional Motions. *J. Am. Chem. Soc.* **2001**, *123*, 6447−6448.
(50) Duvanel, G.; Banerji, N.; Vauthey, E. Excited-State Dynamics of Donor-Acceptor Bridged Systems Containing a Boron-Dipyrromethene Chromophore: Interplay between Charge Separation and Reorientational Motion. *J. Phys. Chem. A* **2007**, *111*, 5361−5369.
(51) Roy, K.; Kayal, S.; Ravi Kumar, V.; Beeby, A.; Ariese, F.; Umapathy, S. Understanding Ultrafast Dynamics of Conformation Specific Photo-Excitation: A Femtosecond Transient Absorption and Ultrafast Raman Loss Study. *J. Phys. Chem. A* **2017**, *121*, 6538−6546.
(52) Drobizhev, M.; Tillo, S.; Makarov, N. S.; Hughes, T. E.; Rebane, A. Absolute Two-Photon Absorption Spectra and Two-Photon Brightness of Orange and Red Fluorescent Proteins. *J. Phys. Chem. B* **2009**, *113*, 855−859.

DOI: 10.1021/acs.jpclett.7b02754
J. Phys. Chem. Lett. 2017, 8, 5878−5883